Dalton Transactions

Accepted Manuscript

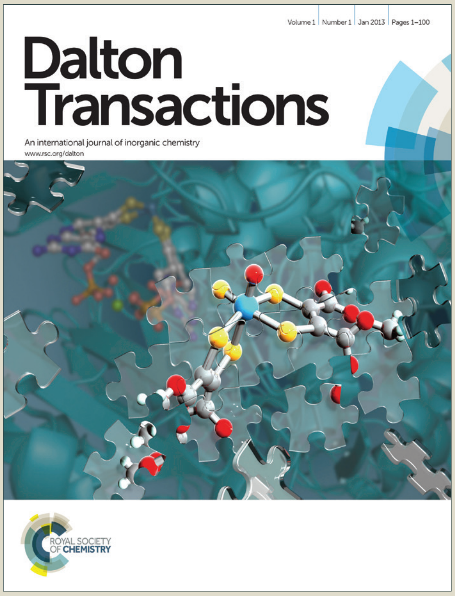

ROYAL SOCIETY OF CHEMISTRY

www.rsc.org/dalton

Dalton Transactions RSCPublishing

ARTICLE

Cite this: DOI: 10.1039/x0xx00000x

Low-temperature reduction of brownmillerite $CaFeO_{2.5}$ in $LaAlO_3/CaFeO_{2.5}$ heterostructures made on $SrTiO_3$

Noriaki Murakami,[a] Daisuke Kan,[a] Noriya Ichikawa[a] and Yuichi Shimakawa[a,b] ,

Received 00th June 2014,
Accepted 00th June 2014

DOI: 10.1039/x0xx00000x

www.rsc.org/

When $LaAlO_3/CaFeO_{2.5}$ thin-film heterostructures made on $SrTiO_3$ were annealed with CaH_2 at low temperatures below 300°C, the brownmillerite $CaFeO_{2.5}$ layer was reduced to $CaFeO_2$ with infinite-layer structure while both the $LaAlO_3$ capping layer and the $SrTiO_3$ substrate remained intact. The reduction behaviour strongly depends on the lattice matching of $LaAlO_3$ to $CaFeO_{2.5}$, suggesting that oxygen ions migrate through the coherently grown $LaAlO_3$ layer of the heterostructure predominantly in the out-of-plane direction. The structural defects near the interface in the relaxed-structure $LaAlO_3$ capping layer prevent the oxygen ions from migrating.

Introduction

Transition-metal ions in oxides can modify their oxidation states and oxygen coordinations. In iron oxides like $CaFeO_x$ the oxidation state of the Fe ions in the perovskite-structure framework changes from Fe^{2+} to Fe^{4+} when the oxygen content x changes from 2 to 3. $CaFeO_2$ has an infinite-layer structure with Fe^{2+} in a nearly square-planar coordination[1,2]. $CaFeO_{2.5}$ has a brownmillerite structure consisting of $Fe^{3+}O_6$ octahedra and $Fe^{3+}O_4$ tetrahedra[3,4], and the simple perovskite $CaFeO_3$ contains corner-sharing $Fe^{4+}O_6$ octahedra[5,6]. Because oxygen ions are incorporated into and released from the perovskite-structure framework during oxidation and reduction of the iron oxide, these phase changes provide us an excellent platform to see oxygen-ion migrations in the oxides[7,8]. Recent experimental results on low-temperature topotactic reactions between $CaFeO_2$ and $CaFeO_{2.5}$ highlighted the fact that such migrations occurred at temperatures below 300°C[9,10].

The oxygen migration in oxide thin films and heterostructures recently attracts much attention[11,12,13]. The low-temperature reduction and oxidation of artificial superlattice thin films also gave us interesting information on the oxygen-ion migration[14,15]. When the brownmillerite/perovskite artificial superlattices $[CaFeO_{2.5}]_m/[SrTiO_3]_n$ were annealed in the presence of CaH_2, $[CaFeO_2]_m/[SrTiO_3]_n$ superlattices formed as the brownmillerite layer was reduced to $CaFeO_2$ with infinite-layer structure and the perovskite layer $SrTiO_3$ was kept intact. The topotactic oxidation of $[CaFeO_2]_m/[SrTiO_3]_n$ to $[CaFeO_{2.5}]_m/[SrTiO_3]_n$ was also observed, confirming the reversible incorporation and release of oxygen ions. The results suggested two possible oxygen-ion migration pathways in the superlattices. If we assume the oxygen ions were released from the thin-film surface because the film thickness (of nanometer order) was much less than the films lateral extent (of centimeter order), they must have passed through the perovskite $SrTiO_3$ layers. On the other hand, since the perovskite $SrTiO_3$ did not change during the reduction, the oxygen ions seemed to migrate along the in-plane direction and to be released from and incorporated at the edges of the films. Since small amounts of oxygen defects, which are difficult to detect in the structure analysis, are easily introduced in $SrTiO_3$ (refs. 16,17), it was difficult to clarify which migration pathway is dominant during the reduction and oxidation of the superlattices.

In this study we have investigated low-temperature reduction of $LaAlO_3/CaFeO_{2.5}$ heterostructures made on $SrTiO_3$ substrates. Instead of using artificial superlattices with $SrTiO_3$ layers, we used a simple heterostructure with a capping layer of perovskite $LaAlO_3$, which is pretty stable against a reducing atmosphere. We found that the reduction behaviour of the $CaFeO_{2.5}$ layer strongly depends on the lattice matching between the $CaFeO_{2.5}$ and $LaAlO_3$ layers. Based on our experimental results, we discuss how important the $CaFeO_{2.5}/LaAlO_3$ interface is in the oxygen-ion migration in the thin-film heterostructures.

Experimental

$CaFeO_{2.5}$ (hereafter referred to as CFO2.5) thin films were prepared on cubic (001) $SrTiO_3$ (STO) substrates by pulsed laser deposition using a KrF excimer laser (COHERENT COMPex-Pro 205 F, $\lambda = 248$ nm and a fluence of 4.1 J/cm^2). The $LaAlO_3$ (LAO) capping layer on each was then deposited under the same conditions but with a laser fluence of 2.9-6.1 J/cm^2. The substrate temperature was kept at 650°C and oxygen partial pressure during the deposition was 10^{-5} Torr. The structures of the deposited films were evaluated by X-ray diffraction (XRD) measurements (PANalytical X'Pert

MRD). Film thickness deposited in the present study ranged from 15 to 60 nm for CFO2.5 and from 6 to 15 nm for LAO.

The heterostructures thus obtained were then reduced with CaH_2 at 240°C. The sample specimens and CaH_2 (0.3 g) were put together in a tube under an Ar atmosphere, sealed, and kept in a furnace at 240°C for 6-72 hours. After reduction, each sample was rinsed with 2-butanone to remove residual products and unreacted CaH_2 on the surface.

Results and Discussion

2θ-θ XRD patterns for as-prepared heterostructures with 30-nm-thick CFO2.5 layers and 12 nm-thick LAO layers that were deposited with 2.9 and 4.1 J/cm^2 laser fluences are shown in Figs. 1(a) and (b), respectively. We see in each heterostructure (0 0 *l*) reflections of the LAO capping layer, (0 2*k* 0) reflections of the CFO2.5 layer, and (0 0 *l*) reflections of the STO substrate, confirming that both LAO and CFO2.5 layers grow epitaxially with (001) and (010) orientations, respectively, on the (001) STO substrate. As discussed in previous reports[9,10], the lattice mismatch between CFO2.5 and STO produced the (010) orientation of the brownmillerite CFO2.5 grown on the STO substrate.

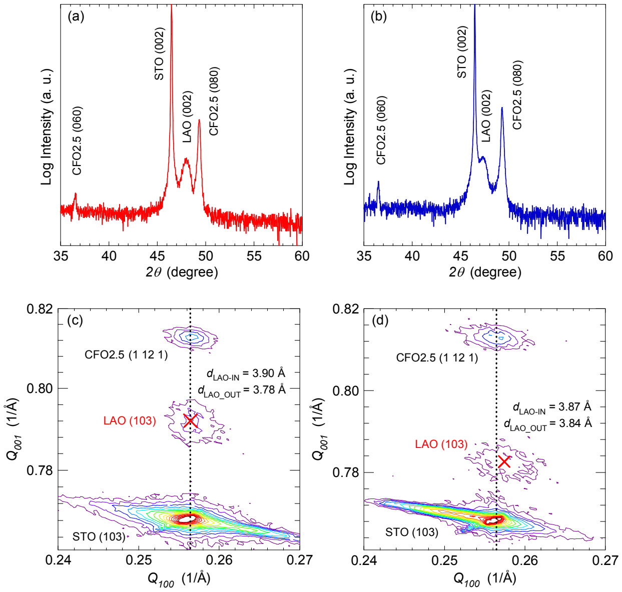

Fig. 1 2θ-θ XRD patterns of LAO/CFO2.5/STO heterostructures in which the LAO was deposited with a laser fluence of (a) 2.9 or (b) 4.1 J/cm^2. (c) and (d): XRD intensity reciprocal space mapping around the (103) STO reflection of the heterostructures whose 2θ-θ XRD patterns appear in (a) and (b).

Note that the position of the LAO reflection differs between the two heterostructures, although that of the CFO2.5 reflection is essentially the same for each heterostructure. XRD intensity reciprocal space mapping around the STO (103) reflection (Figs. 1(c) and (d)) reveals that the in-plane lattice of CFO2.5 is fixed at the lattice of the STO substrate in each heterostructure, indicating that the brownmillerite CFO2.5 layer grows coherently. For the heterostructure with the LAO layer deposited with 2.9-J/cm^2 fluence, the (103) LAO reflection is seen in the same position along the Q_{100} direction as those of the CFO2.5 layer and substrate reflections (Fig. 1(c)), indicating that the capping LAO layer also grows coherently. The out-of-plane lattice parameter of LAO is 3.78 Å, and the LAO lattice is also coherently grown and strained. On the other hand, the (103) LAO reflection for the heterostructure with the LAO layer deposited with 4.1 J/cm^2 fluence appears at a position with a Q_{100} larger than those of the positions of the CFO2.5 layer and substrate reflections (Fig. 1(d), suggesting that the LAO lattice is relaxed from the CFO2.5/STO heterostructure lattices. The in-plane and out-of-plane lattice parameters of LAO are 3.87 and 3.84 Å, both of which are close to the lattice parameter of bulk LAO. Because the laser fluence strongly influences cation compositions in oxide thin films[18,19,20], the observed difference in the lattice parameters probably results from slightly different cation compositions in the LAO layers. Note that the crystal quality of the CFO2.5 layer is the same in both of these heterostructures, regardless of whether the capping LAO layers are strained or relaxed.

The XRD patterns obtained after the heterostructures whose XRD patterns are shown in Figs. 1(a) and (b) were treated with CaH_2 for 24 hours at 240°C are shown in Figs. 2(a) and (b), where one sees that the XRD profiles of the LAO layers in both heterostructures were not changed by the reduction. We found, however, that reduction changed the brownmillerite CFO2.5 layer in the heterostructure with the coherently grown LAO capping layer into $CaFeO_2$ (CFO2). After the reduction for 24 hours, XRD intensities of the CFO2.5 peaks are decreased and CFO2 peak is evident (Fig. 2(a)). By the reduction for more than 48 hours, the CFO2.5 layer in the heterostructure is completely reduced to CFO2 and no peak originated from the deposited CFO2.5 is evident (Fig. 2(c)). The observed XRD pattern of CFO2 is quite similar to that obtained from CFO2.5 without the LAO capping layer reduce for 72 hours (Fig. 2(d)). Thus the CFO2.5 layer is completely reduced to CFO2 in the heterostructure with the coherently grown LAO capping layer. The conversion of CFO2.5 into CFO2 is clearly seen in Fig. 3, where the CFO2.5 (080) reflection intensity is plotted as a function of the reduction time. The XRD pattern of the CaH_2-treated heterostructure with the relaxed LAO layer, in contrast, is similar to that of the as-prepared one and has only a tiny CFO2 peak (Fig. 2(b)). No significant decrease in the CFO2.5 diffraction peak intensity was observed even after 48 hours reduction.

The reduction behaviors of the heterostructures strongly suggest that the oxygen-ion migration during the CaH_2 reduction occurs predominantly in the out-of-plane direction rather than the in-plane direction. Because the crystal quality of the CFO2.5 layers in the two heterostructures is essentially the same, if oxygen ions migrate mainly along the in-plane directions, the reduction behaviors of the brownmillerite layers would not be influenced by the difference in the LAO capping layers. Therefore the oxygen ions pass through the thin layer of coherently grown LAO. Given that lattice relaxation often introduces extended defects like dislocations and planar defects in the films[21,22,23], such defects appear to prevent the oxygen ions from migrating or hopping into the neighboring sites in the thin-film capping layer. As also shown in Fig. 3, the reduction time depends on the lattice parameter of the deposited capping LAO layer, implying that the amount of the defects affects the oxygen migration behavior.

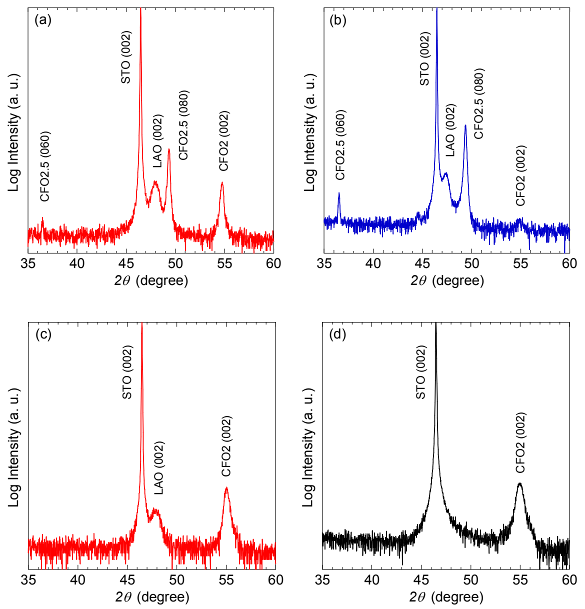

Fig. 2 (a, b) 2θ-θ XRD patterns of the heterostructures whose 2θ-θ XRD patterns appear in Figs.1 (a) and (b) after the reduction with CaH_2 for 24 hours. (c) 2θ-θ XRD pattern of the heterostructure with the coherently grown LAO capping layer reduced for 72 hours, and (d) that of CFO thin film without the LAO capping layer reduced for 12 hours.

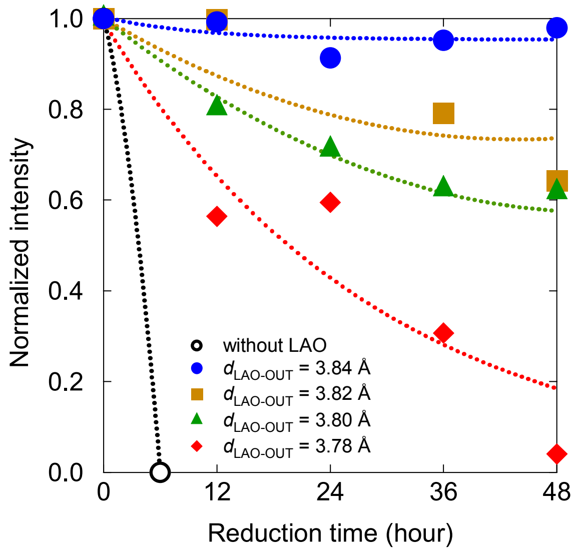

Fig.3 CFO2.5 (080) diffraction intensity as a function of reduction time for LAO/CFO2.5 heterostructures with different lattices of the LAO capping layer. The plotted intensities are normalized by the intensity for the as-prepared heterostructure. The result without a capping layer is also plotted for comparison.

It is important to note that for the heterostructure with the strained LAO, the reaction time needed to complete the reduction from the brownmillerite CFO2.5 phase to the CFO2 phase is more than eight times longer than that for the CFO2.5 without the capping layer. In case of no capping layer, the oxygen ions are directly released from the CFO2.5 surface, the results indicate that the oxygen-ion migration in the CFO2.5 layer is not the rate-limiting process. We have therefore investigated influence of the strained LAO layer thickness on the reduction of the brownmillerite layer. Figure 4 shows the reduction-time dependent change of the CFO2.5 (080) reflection intensity for the heterostructures with 9- and 15-nm-thick strained LAO layers, both of which were grown with the same laser fluence. We found that CFO2.5 was almost reduced after 36 hours regardless of the LAO layer thickness. This means that oxygen-ion migration in the LAO layer is not the rate-limiting process either and thus that the kinetics of the reduction in the heterostructures are probably determined by the migration across the LAO/CFO interface. Since the lattice parameter of the LAO layer strongly affects the reduction behavior of CFO2.5 in the heterostructure, structural defects including slight cation off-stoichiometry near the LAO/CFO interface should play an important role in the oxygen-ion migration during the reduction reaction.

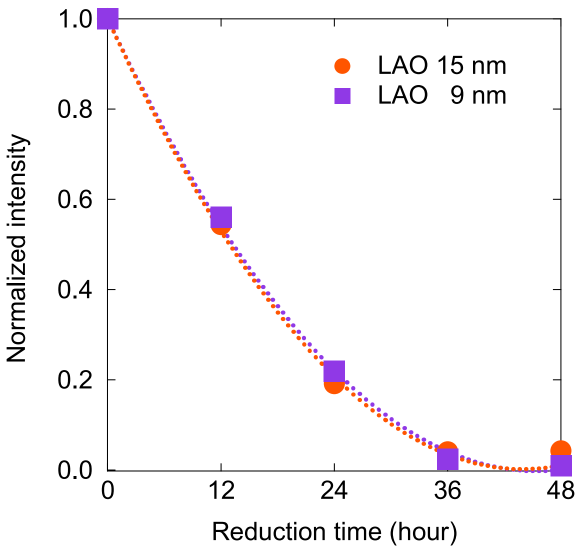

Fig. 4 CFO2.5 (080) diffraction intensity as a function of reduction time for the LAO/CFO2.5 heterostructures with 9- and 15-nm-thick LAO capping layers, both of which were grown coherently on 60-nm-thiock CFO2.5 thin films. The plotted intensities are normalized by the intensity for the as-prepared heterostructure.

Conclusions

$LaAlO_3$ and $CaFeO_{2.5}$ thin films were grown by pulsed laser deposition, and the LAO/CFO2.5 heterostructures thus obtained were treated with CaH_2 at low temperatures below 300°C. The brownmillerite CFO2.5 layer in the heterostructures was reduced to a layer of CFO2 with infinite-layer structure. The time needed to reduce the CFO2.5 in the heterostructures to CFO2 depended on the lattice matching of the capping layer LAO to CFO2.5, and the results suggest that the oxygen ions migrate through the coherently grown strained LAO layer of the heterostructures predominantly in the out-of-plane direction. When the LAO capping layer includes structural defects, oxygen ions cannot migrate in the LAO layer and the heterostructure with CFO2.5 remains intact. The oxygen-ion release through the strained LAO layer is not influenced by the thickness of the LAO capping layer, so the kinetics of the oxygen-ion migration is determined by the LAO/CFO2.5 interface. The present experimental results revealed the importance of lattice relaxation at the interface in the oxide heterostructure with regard to oxygen-ion migration behaviour and should facilitate the development of low-temperature oxide-ion conduction devices.

Acknowledgements

This work was partially supported by a Grant-in-Aid for Scientific Research (Grant Nos. 24760009 and 24540346) and a grant for the Joint Project of Chemical Synthesis Core Research Institutions from the Ministry of Education, Culture, Sports, Science and Technology of Japan. The work was also supported by the Japan Science and Technology Agency, CREST and the Murata Science Foundation.

Notes and references

[a] Institute for Chemical Research, Kyoto University, Uji, Kyoto 611-0011, Japan

[b] Japan Science and Technology Agency, CREST, Uji, Kyoto 611-0011, Japan

1. C. Tassel, T. Watanabe, Y. Tsujimoto, N. Hayashi, A. Kitada, Y. Sumida, T. Yamamoto, H. Kageyama, M. Takano, and K. Yoshimura, *J. Am. Chem. Soc.* 2008, **130**, 3764–3765.
2. C. Tassel, J. M. Pruneda, N. Hayashi, T. Watanabe, A. Kitada, Y. Tsujimoto, H. Kageyama, K. Yoshimura, M. Takano, M. Nishi, K. Ohoyama, M. Mizumaki, N. Kawamura, J. Íñiguez, and E. Canadell, *J. Am. Chem. Soc.* 2009, **131**, 221–229.
3. G. J. Redhammer, G. Tippelt, G. Roth, G. Amthauer, *Am. Mineral.* 2004, **89**, 405–420.
4. M. D. Rossell, O. I. Lebedev, G. Van Tendeloo, N. Hayashi, T. Terashima, and M. Takano, *J. Appl. Phys.* 2004, **95**, 5145–5152
5. Y. Takeda, S. Naka, M. Takano, T. Shinjo, T. Takada, and M. Shimada, *Mater. Res. Bull.* 1978, **13**, 61–66.
6. P. Woodward, D. Cox, E. Moshopoulou, A. Sleight, and S. Morimoto, *Phys. Rev. B* 2000, **62**, 844–855.
7. T. Yamamoto, Z. Li, C. Tassel, N. Hayashi, M. Takano, M. Isobe, Y. Ueda, K. Ohoyama, K. Yoshimura, Y. Kobayashi, and H. Kageyama, *Inorg. Chem.* 2010, **49**, 5957–5962.
8. K. Matsumoto, D. Kan, N. Ichikawa, S. Hosokawa, H. Kageyama, and Y. Shimakawa, *Chem. Lett.* 2013, **42**, 732–734.
9. S. Inoue, M. Kawai, N. Ichikawa, H. Kageyama, W. Paulus, and Y. Shimakawa, *Nat. Chem.* 2010, **2**, 213–217
10. Y. Shimakawa, *Bull. Chem. Soc. Jpn.* 2013, **86**, 299–311.
11. H. Jeen, W. S. Choi, M. D. Biegalski, C. M. Folkman, I. C. Tung, D. D. Fong, J. W. Freeland, D. Shin, H. Ohta, M. F. Chisholm, and H. N. Lee, *Nat. Mater.* 2013, **12**, 1057–1063.
12. Y. Xie, M. D. Scafetta, R. J. Sichel-Tissot, E. J. Moon, R. C. Devlin, H. Wu, A. L. Krick, and S. J. May, *Adv. Mater.* 2014, **26**, 1434–1438.
13. M. Kubicek, Z. Cai, W. Ma, B. Yildiz, H. Hutter, and J. Fleig, *ACS Nano* 2013, **7**, 3276–3286.
14. K. Matsumoto, M. Haruta, M. Kawai, A. Sakaiguchi, N. Ichikawa, H. Kurata, Y. Shimakawa, *Appl. Phys. Exp.* 2010, **3**, 105601.
15. K. Matsumoto, M. Haruta, M. Kawai, A. Sakaiguchi, N. Ichikawa, H. Kurata, and Y. Shimakawa, *Sci. Rep.* 2011, **1**, 27.
16. H. Yamada and G. R. Miller, *J. Solid State Chem.* 1973, **6**, 169-177.
17. H. P. R. Frederikse and W. R. Hosler, *Phys. Rev.* 1967, **161**, 822–827.
18. T. Ohnishi, K. Shibuya, T. Yamamoto, and M. Lippmaa, *J. Appl. Phys.* 2008, **103**, 103703.
19. D. Kan and Y. Shimakawa, *Appl. Phys. Lett.* 2011, **99**, 081907.
20. E. Breckenfeld, R. Wilson, J. Karthik, A. R. Damodaran, D. G. Cahill, and L. W. Martin, *Chem. Mater.* 2012, **24**, 331–337.
21. O. Eibl, P. Pongratz, P. Skalicky, and H. Schmelz, *Phys. Status Solidi A* 1988, **108**, 495–502.
22. M. Fujimoto, *J. Cryst. Growth* 2002, **237–239, Part 1**, 430–437.
23. T. Detchprohm, K. Hiramatsu, K. Itoh, and I. Akasaki, *Jpn. J. Appl. Phys.* 1992, **31**, L1454–L1456.